PLOS COMPUTATIONAL BIOLOGY

RESEARCH ARTICLE

Modelling the effects of adult emergence on the surveillance and age distribution of medically important mosquitoes

Isaac J. Stopard[1,2], **Ellie Sherrard-Smith**[3], **Hilary Ranson**[3], **Kobié Hyacinthe Toe**[4,5], **Jackie Cook**[6], **Joseph Biggs**[6], **Ben Lambert**[7☯], **Thomas S. Churcher**[1☯*]

1 School of Public Health, Imperial College London, London, United Kingdom, **2** School of Population Health, University of New South Wales (UNSW), Sydney, New South Wales, Australia, **3** Liverpool School of Tropical Medicine, Liverpool, United Kingdom, **4** Centre National de Recherche et de Formation sur le Paludisme, Ouagadougou, Burkina Faso, **5** Université Joseph KI-ZERBO, Ouagadougou, Burkina Faso, **6** International Statistics and Epidemiology Group, Department of Infectious Disease Epidemiology, London School of Hygiene and Tropical Medicine, London, United Kingdom, **7** Department of Statistics, University of Oxford, Oxford, United Kingdom

☯ These authors contributed equally to this work.
* thomas.churcher@imperial.ac.uk

OPEN ACCESS

Citation: Stopard IJ, Sherrard-Smith E, Ranson H, Toe KH, Cook J, Biggs J. et al. (2025) Modelling the effects of adult emergence on the surveillance and age distribution of medically important mosquitoes. PLoS Comput Biol 21(8): e1013035. https://doi.org/10.1371/journal.pcbi.1013035

Editor: Kimberly M. Pepin, Animal and Plant Health Inspection Service, UNITED STATES OF AMERICA

Received: April 7, 2025

Accepted: July 24, 2025

Published: August 18, 2025

Data availability statement: All code and data is available at https://github.com/IsaacStopard/mos_age_gono_IBM.

Funding: The work was supported by the Bill and Melinda Gates Foundation (INV-078496), the Natural Environment Research Council (NERC; NE/P012345/1) and the UK Medical

Abstract

Entomological surveillance is an important component of mosquito-borne disease control. Mosquito abundance, infection prevalence and the entomological inoculation rate are the most widely reported entomological metrics, although these data are notoriously noisy and difficult to interpret. For many infections, only older mosquitoes are infectious, which is why, in part, vector control tools that reduce mosquito life expectancy have been so successful. The age structure of wild mosquitoes has been proposed as a metric to assess the effectiveness of interventions that kill adult mosquitoes, and age grading tools are becoming increasingly advanced. Mosquito populations show seasonal dynamics with temporal fluctuations. How seasonal changes in adult mosquito emergence and vector control could affect the mosquito age distribution or other important metrics is unclear. We develop stochastic mathematical models of mosquito population dynamics to show how variability in mosquito emergence causes substantial heterogeneity in the mosquito age distribution, with low frequency, positively autocorrelated changes in emergence being the most important driver of this variability. Fitting a population model to mosquito abundance data collected in experimental hut trials indicates these dynamics are likely to exist in wild *Anopheles gambiae* populations. Incorporating age structuring into an established compartmental model of mosquito dynamics and vector control, indicates that the use of mosquito age as a metric to assess the efficacy of vector-control tools will require an understanding of underlying variability in mosquito ages, with the mean age and other entomological metrics affected by short-term and seasonal fluctuations in mosquito emergence.

Research Council (MRC) Project Grant (MR/P01111X/1). IJS, ESS and TSC also acknowledge funding from the MRC Centre for Global Infectious Disease Analysis (reference MR/X020258/1), funded by the United Kingdom MRC. This United Kingdom funded award is carried out in the frame of the Global Health EDCTP3 Joint Undertaking. The funders had no role in study design, data collection and analysis, decision to publish or preparation of the manuscript.

Competing interests: The authors have declared that no competing interests exist.

Author summary

Mosquito-borne diseases, such as malaria and dengue, remain a significant cause of mortality and morbidity. Predicting changes in the spread of these diseases from mosquito data remains a challenge because only older mosquitoes can transmit important mosquito-borne diseases and mosquito abundance measurements can be highly variable. Trials that test the efficacy of vector control tools using measures in both mosquitoes and people have found the metrics are not always consistent. Methods to measure the mosquito age quickly and accurately are in development, and changes in the mosquito age distribution have therefore been proposed as a metric to measure the efficacy of novel vector control tools. We develop mathematical models of mosquito reproduction, development and ageing to show that seasonality in adult mosquito emergence can result in substantial seasonality in the mosquito age distribution and complicate the interpretation of mean mosquito age and other widely used mosquito metrics. Using data from the dominant malaria vector *Anopheles gambiae* we predict that even over short time-scales there is likely to be substantial variability in the abundance and age of wild mosquito populations.

1. Introduction

Entomological surveillance is an important component of mosquito-borne disease control and is regularly used to assess entomological risk and the effectiveness of current and potential future vector control interventions [1,2]. Mosquito abundance, parity (the proportion of mosquitoes that have laid eggs), the proportion of mosquitoes that are infectious and the entomological inoculation rate (rate at which people receive infectious bites) are currently the most widely used metrics. These metrics are, however, difficult to measure accurately [1], with mosquito catches depending on the location and trapping methods [3], and noise in adult mosquito emergence making it difficult to infer changes in transmission [4]. Indeed, epidemiological and entomological end points of vector control trials do not always indicate effects in the same direction [2].

To transmit malaria-causing *Plasmodium* parasites, and numerous arboviruses, mosquitoes must survive the extrinsic incubation period (EIP). For many mosquito-borne diseases the EIP is long relative to mosquito life expectancy [5,6], meaning small changes in the adult mosquito age distribution cause large changes in entomological transmission intensity [7–9]. This explains, in part, why interventions that reduce mosquito survival have been so important to mosquito-borne disease control [7,10,11]. Measuring the age of wild mosquitoes is challenging [12,13]. Historically, the age distributions of *Anopheles* mosquitoes were estimated using morphological methods: the physiological age, for example, was estimated by dissecting mosquitoes and counting the number of dilations at the base of the ovarioles to estimate the number of gonotrophic cycles that the mosquito has survived (Polovodova's technique) [13]. Calendar age can then be approximated by making an assumption about the length of the gonotrophic cycle, which is generally assumed to be about 3 days [14]. Alternatively, calendar age can be measured morphologically by counting the layers of cuticular growth on the inner apodemes, which increase daily [15]. These methods are, however, laborious and require substantial skill, meaning they are impractical to use on a large scale [12]. Novel age grading techniques that measure calendar age using spectroscopic or gene and protein profiling methods are in development [12], and studies employing spectroscopy and

machine learning models have recently demonstrated increases in accuracy [16,17]. Wild mosquito age distribution data may therefore become more available in the future.

Age grading of wild mosquitoes has been proposed as a method to evaluate novel vector control tools that kill adult mosquitoes, as increased mortality could be indicated by a shift in the mosquito age distribution [12]. Although intuitive, this has not been directly observed, either through mechanistic simulation models or in field data, though changes in mosquito parity (a proxy for age) have sometimes been observed [18]. Hypothetically, the age structure of the mosquito population will be driven by changes in both adult mosquito mortality and emergence; during periods of increased emergence, for example, the proportion of young mosquitoes increases, which means the temporal dynamics of mosquito abundance can affect the mosquito age distribution [19]. These processes therefore also affect parity and infection prevalence, which depend on mosquitoes surviving the first gonotrophic cycle or EIP respectively.

Medically important mosquito populations often show seasonal dynamics and spatiotemporal fluctuations [20,21], contributing to seasonal patterns of transmission [22]. Population dynamics can be driven by demographic and environmental processes: vital demographic rates, for example, can change due to changes in environmental variables or intrinsic demographic processes (such as density dependence) [23–25]. Changes in demographic rates can occur at fixed frequencies resulting in seasonal population dynamics (seasonal or periodic forcing). These temporal trends in the population are classed as red when low-frequency, positively autocorrelated changes dominate (for example, high emergence today is likely to be followed by high emergence tomorrow), blue when high-frequency, negatively autocorrelated changes dominate (high emergence today is likely to be followed low emergence tomorrow) and white when no frequency dominates [26]. Empirical temporal abundance data spanning more than 30 years for 123 species indicates that changes in abundance are typically low-frequency, though smaller animals tend to have less red fluctuations [27]. The red frequency of temporal fluctuations in the abundance is commonly attributed to changes in environmental variables, because positive autocorrelation is observed in both the abundance and environmental variable time-series [28]. Species with high growth rates theoretically respond more to the colour of environmental noise, meaning they are more sensitive to differences in the autocorrelation of environmental variables [26,29]. Indeed, anopheline mosquito dynamics show species-specific responses to certain environmental variables, such as rainfall, temperature, humidity, windspeed and land use [21,22,30–34]. Fluctuating mosquito populations in time and space will likely increase the noise in entomological metrics and could explain some of the high variability observed in field data, complicating interpretation [2]. There has, however, been little research on the colour of temporal fluctuations in adult mosquito emergence and the resultant impact on the variability of adult mosquito metrics and age distribution.

In this study we aim to (1) develop a mathematical model of adult mosquito population dynamics that explicitly allows quantification of the mosquito age distribution and parameterise it for the dominant malaria vector *An. gambiae*, (2) investigate how temporal heterogeneity in the age distribution of the mosquito population is affected by differences in the frequency and autocorrelation of fluctuations in mosquito emergence, (3) estimate the observed autocorrelation in the emergence of wild *An. gambiae sensu lato* mosquitoes and predict changes in the age distribution given these changes in emergence, and (4) investigate the impact of vector control on the mosquito age distribution with variable emergence. This work will help interpret wild mosquito age distribution data and guide trial design for novel vector control tools that investigate changes in entomological metrics, in particular mosquito age distributions.

2. Results

2.1. Mosquito emergence can drive patterns in mosquito metrics

We develop a stochastic individual-based model (IBM) of female adult *An. gambiae* mosquito dynamics that tracks individual mosquito emergence, parity, ageing and mortality over discrete time steps. In this model, mosquito survival, emergence and gonotrophic cycle duration are treated as random variables represented by probability distributions, and the model is parameterised assuming a constant per-capita mosquito mortality rate. In this model adult mosquito emergence is stochastic; the numbers of adult mosquitoes emerging varies daily following a Poisson distribution ($o_t \sim \text{Poisson}(\lambda_t)$) and the mean emergence rate (λ_t) can vary temporally, with the variation characterised by either (a) different frequencies (represents the outcome of periodic forcing, captures the number of transmission seasons per year) or (b) different levels of temporal autocorrelation (correlation in emergence between successive days). This model is used to estimate both temporal changes in mosquito abundance, parity and the age distribution of a group of adult mosquitoes over time (Fig 1A). The parity and age distribution of mosquitoes is assessed from all simulated mosquitoes with approximately 200 mosquitoes initially and we calculate the metrics using all simulated mosquitoes.

Stochastic processes cause noise in the mosquito age distribution, but given perennial dynamics (a constant mean adult mosquito emergence rate) the modelled age distribution and mean age of the mosquitoes are observed to be relatively stable over time (Fig 1A and 1B). In contrast, when mean adult mosquito emergence varies seasonally the model produces seasonal variability in the mosquito age distribution, with it shifting towards younger mosquitoes when the abundance is increasing, and older mosquitoes when the abundance declines (Fig 1A and 1B). The range in the mean daily mosquito age over a single year is substantial; for example, it varied over the year between 4.1 and 14.0 days in simulations with a one peak transmission season and 5.3 and 8.8 days in those with perennial dynamics (Fig 1B). Similar patterns are seen in the proportion of mosquitoes that are parous (Fig 1B). Greater variability is predicted in the proportion of mosquitoes at least 10 days old, analogous to the proportion of mosquitoes capable of being infectious with malaria, fluctuating between 8% to 51% in all simulations with seasonal emergence, and 17% and 39% in those with perennial dynamics (Fig 1B). We calculate the coefficient of variation (ratio of the standard deviation to the mean, CV) of the temporal changes in the different entomological metrics (Fig 1C). In simulations with perennial dynamics the CV of both mosquito abundance and the mean mosquito age are similar irrespective of the time frame considered (either the complete primary transmission season [half year] or the two weeks when abundance peaks) (Fig 1C). When the time-frame considered includes the complete primary transmission season (180 days) seasonality in mosquito emergence increases the CV in the mosquito abundance, but not the other metrics (Fig 1C). When the time frame considered is shorter (the two-weeks that includes the peak of transmission) the CV in mosquito abundance is less and the CV for the proportion of mosquitoes older than 10 days is the most variable metric (Fig 1C). To assess the robustness of these results, we investigated the sensitivity of temporal changes in the mean mosquito age to differences in the (1) frequency (assuming a medium amplitude) (S1 Fig) and (2) amplitude (assuming one peak per year) of fluctuations in the mean adult mosquito emergence rate (S2 Fig). The CV in the mean daily mosquito ages was most sensitive to larger amplitude changes in adult mosquito emergence at low to medium frequencies (approximately 5–10 radians per year) (S3 FigA and S3 FigB).

Age grading has been proposed as a method of estimating the mosquito mortality rate. We investigate how variable emergence might bias these estimates by fitting a survival model

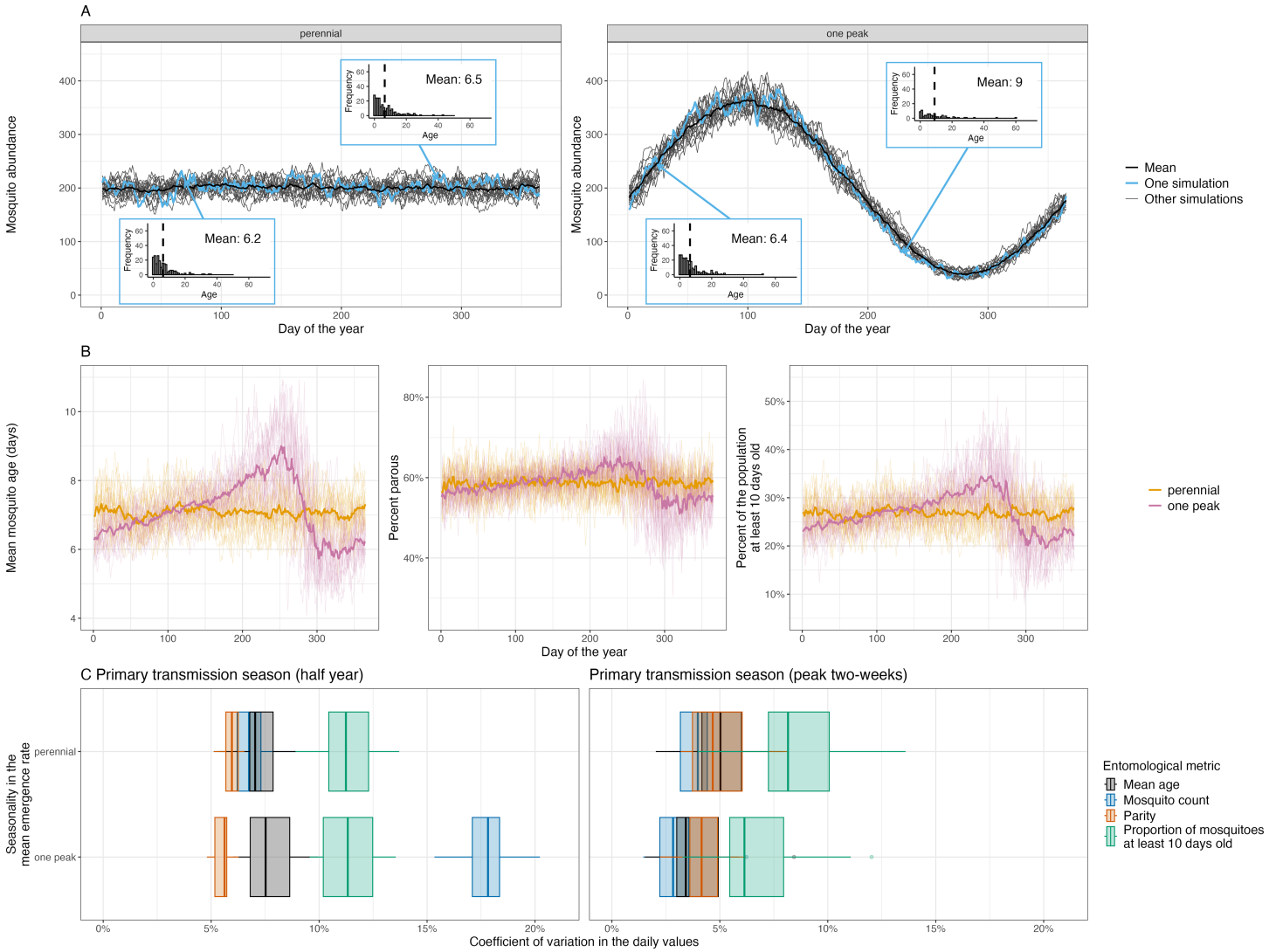

Fig 1. Seasonal dynamics in mosquito emergence changes the adult mosquito age distribution. (A) The temporal dynamics in mosquito abundance from single simulations assuming the mean adult, female mosquito emergence rate is either time-invariant (perennial dynamics) or follows a sine wave with a single period per year (one peak dynamics). For one of these simulations (highlighted in blue) we presented the predicted mosquito age distribution on two different days; in these histograms the dashed vertical line indicates the mean age. For the seasonal setting the day selected was when the mosquitoes abundance was increasing or decreasing. In the main plots the thicker black line show the means abundance value from all the simulations. The initial number of mosquitoes in the group was approximately 200. For all plots, the model was simulated with an overall mean emergence rate of 26.4 per day over the year (equal to the mean number of mosquitoes that die per day). For the seasonal simulations the mean emergence rate was assumed to vary at a frequency of 1 radian per year (giving an angular frequency 2π per year), with an amplitude of 20 mosquitoes. (B) shows how the mean mosquito age, percent of mosquitoes that are parous or at least 10 days old varied with time given different seasonal patterns in mosquito emergence. The thin lines show the results from a single simulation and the thicker lines show the mean values of all the simulations. (C) Shows how the coefficient of variation (ratio of the standard deviation to the mean) over the primary transmission season (day 1 to 180) and two-week centred on the peak transmission season varies depending on the entomological metric used. Box plots show the variability between different simulations, with the central values being the median, hinges showing the 25th and 75th percentiles, and the whiskers indicating the smallest or largest values no further than 1.5 interquartile ranges from the hinges.

https://doi.org/10.1371/journal.pcbi.1013035.g001

to the simulated mosquito age distributions from each day. Individual mosquito survival is treated as a Bernoulli trial in the model, with the probability a mosquito dies assumed to be constant with time. This model assumes that the mosquito population is stable and the age distribution mirrors the life time distribution. This is not the case in the simulations with seasonal emergence, meaning the fitted per-capita mortality rates were biased, the values from all

simulations, for example, varied between 0.11 and 0.19 over the year given perennial changes in mosquito emergence and 0.07 and 0.25 given a one peak transmission season (S4 Fig). These methods can therefore not accurately estimate mortality in seasonal settings.

2.2. Estimated changes in the emergence of wild mosquitoes

Temporal changes in the adult mosquito emergence rate can be characterised by the level of autocorrelation. Theoretically, the lag-1 autocorrelation can be positive ($h>0$), meaning there is positive correlation between the rate adults emerge on subsequent days, neutral ($h = 0$), or negative ($h<0$), indicating that if the abundance of emerging adults is high one day it is likely to be low the next (S5 FigA). This range of temporal autocorrelation is explored with the model to see how the autocorrelation influences variability in the mosquito abundance (S5 FigB) and age distribution (S5 FigC). Hypothetically, positive autocorrelation (red fluctuations, high seasonality) increase the variability in daily estimates of the mean mosquito age over a single year more than negatively autocorrelated (blue) fluctuations (S5 FigC, S6 Fig and S7 Fig).

To estimate changes in the emergence of wild mosquitoes, we fit a simplified ordinary differential equation (ODE) version of the adult mosquito model, which models changes in mosquito abundance assuming a time-varying daily mosquito emergence rate (characterised by a lag-1 autoregressive model) and constant mortality rate, to previously published, temporally disaggregated experimental hut trial (EHT) data from Burkina Faso [35] (Figs 2A and 2B). The ODE model posterior mean emergence rate, lag-1 autoregressive model standard deviation, and overdispersion parameter values are shown in S8 Fig. The coefficients of determination (R^2) of the model fits are 8.4% for Tengrela and 10.0% for Vallée du Kou 5 (VK5). The estimated posterior autocorrelation parameters in the daily emergence rate exceed zero, indicating that mosquito emergence is positively autocorrelated (Fig 2C).

To estimate potential changes in the age distribution, the estimated initial numbers of mosquitoes and daily adult mosquito emergence rates are multiplied by the number of experimental huts and used as parameter inputs within our IBM. The resultant simulated changes in mosquito abundance and the age distributions of the mosquito population during the EHTs are shown in Figs 2D and 2E respectively. Despite the short duration of the EHTs there is clear predicted temporal variability in the mosquito age distributions, with the predicted mean mosquito age varying between 4.6 and 10.9 days in the Tengrela EHT and 3.0 days and 10.9 days in the VK5 EHT, with the mosquitoes being younger during the start of the EHT and older towards the end (Fig 2E).

2.3. Investigating the impact of interventions on mosquito age

To assess the effects of insecticide treated bed nets (ITNs) on the age distribution of the mosquito population, we develop a discrete time stochastic version of a well established compartmental, differential equation model of seasonal larval and adult mosquito population dynamics that includes vector control interventions [36,37]. We adapt this model to track mosquito age by transitioning mosquitoes between different age compartments with each discrete time step (dt = 1 day). We simulate seasonality in mosquito population dynamics (implemented through changes in the larval carrying capacity) based on either (1) rainfall for the Cascades region of Burkina Faso or (2) perennial dynamics (Fig 3A). Pyrethroid-only ITNs are introduced when the mosquito population is either increasing or decreasing. The model indicates ITNs consistently decrease the mean mosquito age, irrespective of the implementation timing (Fig 3B). For example, in a perennial setting, ITNs are predicted to reduce mosquito abundance by 63% (mean value from all simulations, ranges from 50% to

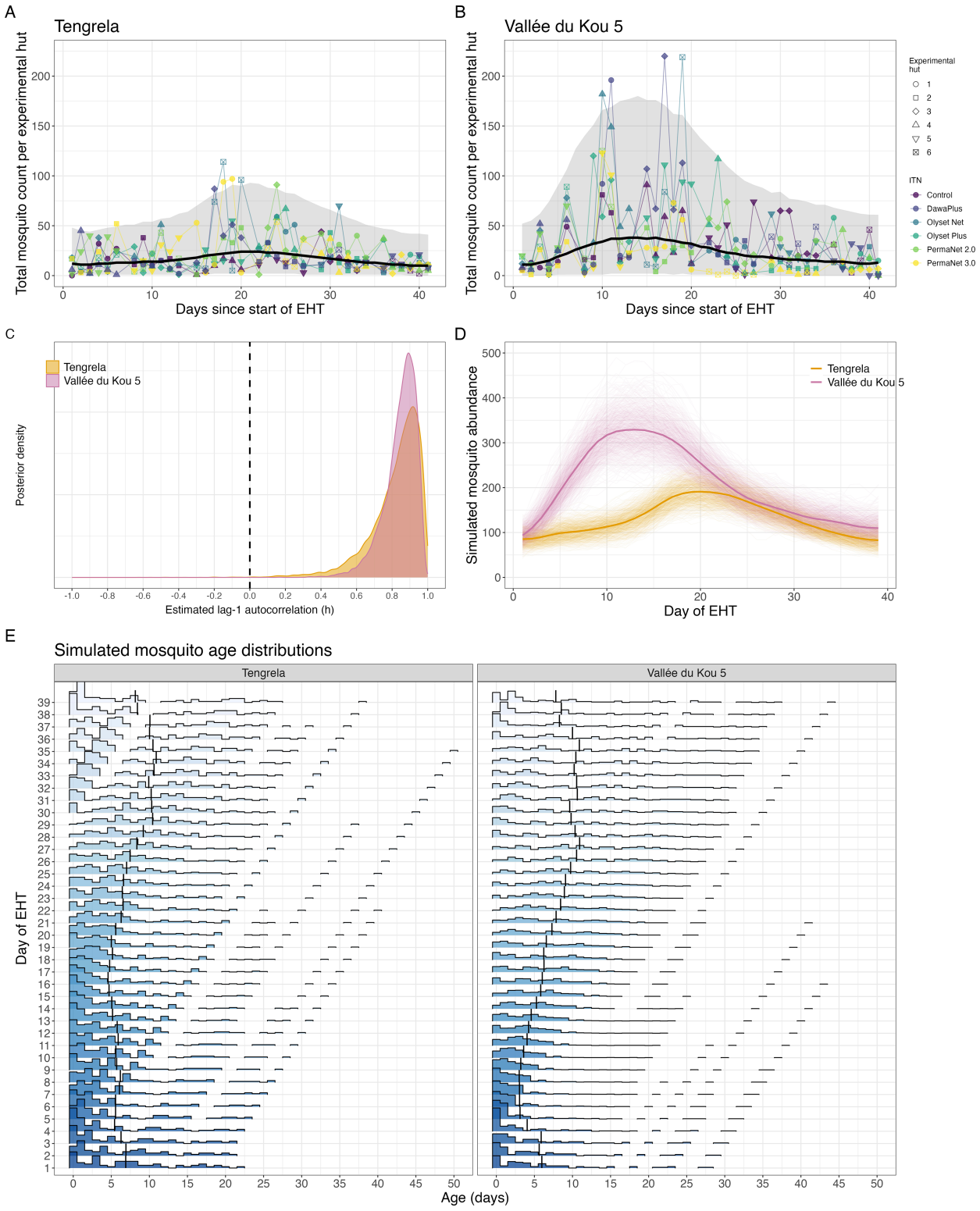

Fig 2. Changes in the adult mosquito age distribution predicted in experimental hut trials (EHTs). (A) and (B) show the numbers of mosquitoes captured during the EHTs. The black line shows the number of mosquitoes predicted by the ordinary differential equation (ODE) model with the 95% credible intervals indicated by the shaded area. The ODE model is fitted to data from all experimental huts and gives the number for a single experimental hut. (C) The estimated autocorrelation in the adult mosquito emergence rate (λ_t) in the ODE, assuming a constant per-capita mortality rate. (D) The simulated mosquito abundance in the individual based model using the fitted λ_t values as the mean

of the Poisson distributed numbers of adult mosquitoes emerging. The initial numbers of mosquitoes (M_0) and λ_t values are multiplied by the number of experimental huts to give the total abundance across all experimental huts. The thin lines show the values for 750 simulations given different samples from the posterior parameter values. The thick lines shows the mean simulated abundance. (E) The predicted changes in the mosquito age distributions during the EHT for a single random simulation with one random draw from the posterior λ_t estimates. The vertical line shows the mean simulated mosquito age. EHT data was obtained from [35].

https://doi.org/10.1371/journal.pcbi.1013035.g002

75%) after the first month and reduce the mean age from 7.2 days (mean value from all simulations, ranges from 6.1 to 8.4 days in all simulations) to 2.2 days (ranging from 1.6 to 3.4 days, a drop of 69% [range in all simulations: 55-80%]). Similar patterns are seen if the intervention is implemented early in the transmission season, reducing mosquito abundance by 62.2% (range from 50.4% to 71.4% in all simulations) and reducing the average age from 6.4 days (5.8-7.3 days in all simulations) to 2 days (1.4-2.7 days in all simulations, a drop of 68.7% [58.3-76.7% in all simulations]). However, implementing the same intervention towards the end of the transmission season the model predicts a 63.8% (ranging from 52.3 to 74.7% in all simulations) reduction in mosquito abundance after the first month, with the average age reducing from 11.4 days (ranging from 8.2 to 15.3 days in all simulations) to 2.9 days (1.5 - 4.3 days in all simulations, a drop of 74.5% [62.1-88.2% in all simulations]). When the mosquito abundance is decreasing the mean age increases and once ITNs are implemented the magnitude of these fluctuations decreases (Fig 3B). This means that if ITNs are rolled out when the mosquito population is decreasing, the effect of the ITNs on the mean adult mosquito age may appear larger than if ITNs (or other vector control) are rolled out as vector abundances increases (Fig 3C). This demonstrates the importance of understanding age structure dynamics to interpret intervention effects and the importance of when sampling is conducted.

3. Discussion

There has been substantial research into the theoretical importance of the mosquito age distribution for disease transmission [7,8] and consequently also methods to estimate the age of a mosquito [12,13,16,17,39]. Here, we use mathematical models to demonstrate how the age of mosquitoes could change in response to variable emergence (noise and seasonal trends in abundance) and the use of control interventions. The model is parameterised using field data from the most important vector of malaria and demonstrates how conventional mosquito control is likely to cause substantial shifts in the age distribution of the mosquito population. Simulations like these can be used to support the development of mosquito age grading methods by demonstrating the level of precision needed for a technique to have practical use as surveillance tools. The work highlights that interpreting changes in the age distribution of wild mosquitoes is complex as there is likely to be considerable noise and seasonal trends in the age distribution of mosquitoes even over short time-scales. Assuming all else is equal, the IBM of *An. gambiae* population dynamics predicts that annual seasonality (low frequency, highly autocorrelated changes in mosquito emergence), such as those identified in Burkina Faso, will likely cause the greatest temporal variation in mosquito ages. It has been suggested that age structures could be used to assess the impact of vector control interventions by evidencing different distributions in control and treatment settings during trials [12]. This modelling exercise suggests that we would need sufficient *a priori* information about seasonality to interpret results for this purpose. Indeed, in our compartmental model with vector control, if the changes in the age distribution are just measured pre- and post-intervention, the apparent change in the mosquito age distribution due to ITNs can be affected by when the ITNs are distributed relative to the transmission season. Interpreting changes in the mosquito age

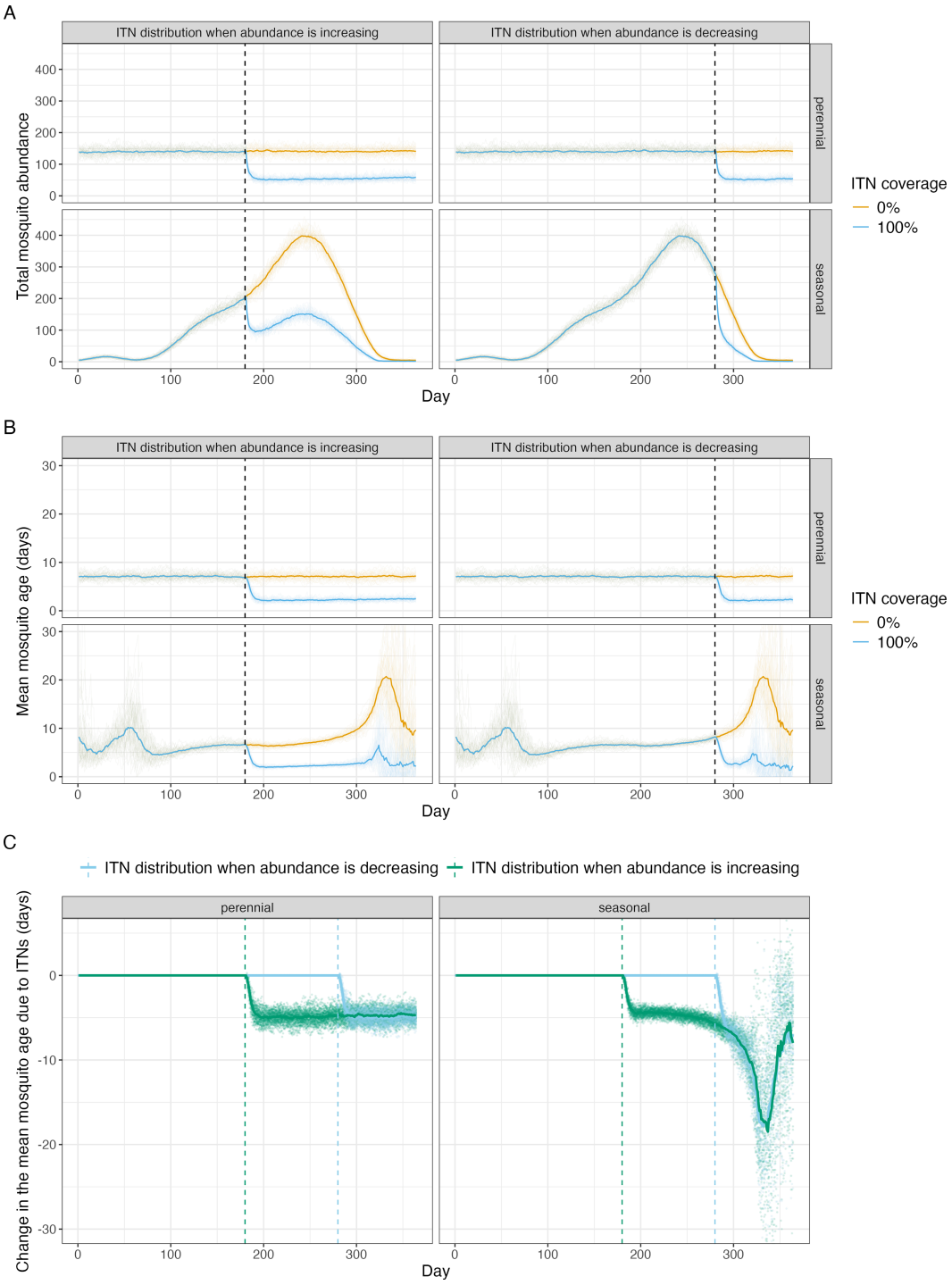

Fig 3. The projected effects of insecticide treated nets (ITNs) on the age distribution of the mosquito population. Mosquito population dynamics are simulated using a state-space version of an established compartmental mosquito population model [36,38], with seasonality determined by either (1) perennial dynamics or (2) rainfall in Cascades region of Burkina Faso. Panels (A) shows estimates of mosquito abundance, (B) the mean age of the mosquito population, and (C) the reduction in the mean age of mosquito populations due to the use of ITNs. In A-B the yellow lines indicate simulations with no ITNs, with blue lines denoting populations where ITNs are deployed at the vertical dashed line (day 180 of the year for the panels titled "ITN distribution when abundance is increasing" and day 280 in panels titled "ITN distribution when abundance is decreasing"). Multiple stochastic realisations of the model are shown, with the mean value denoted by the thicker line.

https://doi.org/10.1371/journal.pcbi.1013035.g003

distribution will therefore need to carefully consider the timing of sample collection and be aware of seasonality and differences in the local fine-scale variability between experimental sites depending on, for example, proximity to breeding habitats [8], which could bias results. However, simulations suggest that the variability in the mean age of mosquitoes is likely to be less than that observed in entomological metrics currently used, such as abundance and infectiousness (Fig 1C). This finding leads on from previous work that demonstrated the uncertainty around these conventional metrics caused by variable mosquito emergence [4]. This variability is likely to be impeding the statistical power of cluster randomised control trials with entomological endpoints. Models like the IBM presented here could be parameterised with field data to allow optimisation of sampling strategies and the generation of robust power calculations. For example, this work demonstrates considerable nightly variability in emergence in Burkina Faso, so mosquito collection over two nights apart may give a more reliable estimate of mosquito abundance, parity, sporozoite prevalence and mean age than samples collected over two consecutive nights. Further analysis of field data is needed to generate guidelines for improving the precision of entomological sampling.

An important finding is that over the time-frames of EHTs there may be substantial changes in the mosquito age distribution due to natural variability in the mosquito population. The R^2 values of the ODE model fits were, however, low. A limitation is that we have not parameterised the stochastic components of the model at the experimental hut level [40], which might understate variability in the age structure. In the EHTs, different insecticide treated nets (ITNs) were rotated around the experimental huts and we are interested in the autocorrelation in emergence of the surrounding mosquito population, so ignored experimental hut level variation due to differences in experimental hut, sleeper or ITN. The R^2 is likely to be improved by accounting for these differences but because ITNs and sleeper are rotated between experimental huts there are insufficient samples to quantify how the fitted seasonal trends could vary with these variables. We fitted the ODE model to the EHT data assuming the mosquito counts followed a negative binomial distribution to account for greater variance due to the sampling. Further detailed sampling of datasets from wild mosquitoes will be needed to explicitly fit this stochasticity and compare metrics.

We parameterised our model for *An. gambiae*, however, due to similar mechanisms these findings are likely to be relevant to other important vectors of mosquito-borne diseases. Sampled mosquito abundance for other mosquito species has been shown to vary at a range of frequencies: the Fourier transforms of daily light trap data for *Aedes vexans* and *Culiseta melanura* sampled over nine years indicate temporal changes in mosquitoes occur at frequencies corresponding to periodicities between two days and multiple years [41]. It has been suggested that generation times of mosquitoes mean that high frequency fluctuations in mosquito abundances of timescales of less than one month are, however, more likely to be due to behavioural responses [41], though care should be taken extrapolating between species due to differences in ovipostion behaviour and the type of breeding habitats.

The modelling exercise made a number of simplifying assumptions. First, it only considers heterogeneity in the emergence of adult mosquitoes and there are likely to be many other sources of variability that will impact mean entomological metrics and estimates and their associated uncertainty. For example, many mosquito demographic processes such as blood-feeding and mortality are likely to vary daily given local environmental conditions. This is likely to substantially increase the heterogeneity of different metrics outlined in Fig 1 and should be considered in sample size calculations. We do not consider biases in the trapping methodology, which could be substantial (particularly at young mosquito ages) and is likely to bias mean age, parity and infectiousness estimates. Second, in the IBM the way we model mosquito emergence means we assumed that increases in the sampled adult mosquito

population due to aestivation and migration are equivalent to newly emerging adults (aged zero). Adult mosquito dispersal and the spatial distribution of larval habitats can, however, also influence population dynamics [42]. The age distribution of migrating mosquitoes is also, theoretically, important for mosquito infection dynamics: assuming a gradient in the mosquito age distribution with distance from larval habitat, for example, mean sporozoite prevalence would increase with dispersal distance [19]. When using the population-level emergence rate estimated from the EHTs to simulate changes in the mosquito age distribution we assumed all mosquitoes came from the same breeding site. Theoretically, the portfolio effect could, however, increase the stability of aggregate mosquito abundance due to the statistical averaging of stochastic fluctuations in the emergence of mosquitoes from different breeding sites [43]. Within the compartmental model we have accounted for potential feedback between the mosquito population size, age distribution and mosquito emergence, though many of the environmental and density-dependent processes governing mosquito emergence remain unclear so the reliability of the immature mosquito model needs further validation. In all models, we assumed a constant background per-capita age-independent mortality rate. Although age-dependent *Anopheles* mortality is observed in the laboratory [5,44]; in the field where mosquitoes have much shorter lifespans senescence is likely to be less important [45]. Using Povolodova's method, for example, Gillies & Wilkes [39] found a relatively constant mortality rate between mosquitoes with different physiological ages up to approximately the 7^{th} gonotrophic cycle. A meta-analysis of mark-release-recapture studies found little evidence of age-dependent mortality in multiple mosquito genera [46]. Mosquito mortality is, however, also strongly temperature and humidity dependent in the laboratory [5,47], which we do not account for. There is empirical evidence for temporal variability in mosquito mortality in wild mosquitoes; Ngowo et al., for example, fitted a state-space model to temporal abundance data of multiple *An. funestus* life stages finding both the fitted survival and fecundity varied temporally [48]. Mark-release-recapture studies of male *An. gambiae*, however, found little effect of seasonality on mosquito mortality [49]. Differences in field and laboratory findings may exist due to mosquito resting behaviour and thermal avoidance [50–53], meaning the relationship between mosquito mortality and temperature, particularly the critical thermal limits, in the field remains an important question. Mosquito age distribution data from wild mosquitoes could therefore help identify the relative inputs of these different mechanisms, but our work demonstrates that interpreting changes in the age distribution of mosquito populations will require a mechanistic model that explicitly accounts for changes in both emergence and mortality. Briet [54], for example, developed methods for estimating adult mosquito mortality rates from parity data whilst accounting for differences in emergence. The model we develop could be fitted to a combination of age structure and abundance of different mosquito life stages to help (1) understand the importance of different mechanisms and (2) estimate sample sizes required to power studies investigating changes in mosquito mortality.

4. Methods

4.1. Data

EHT data are obtained from a single previously published study that carried out EHTs in both the villages of Tengrela and VK5 in the Cascades Region of Burkina Faso [35]. EHTs are an assay used to assess the entomological efficacy of vector control tools; volunteers rest within specially designed house-like structures with different interventions applied, all mosquitoes that enter the experimental hut are trapped and the numbers alive and dead are counted at the beginning of each day [40]. We analyse data for mosquitoes identified as *An. gambiae s. l.*,

though *An. coluzzi* was the only species identified by polymerase chain reaction (PCR) in a subset of these mosquitoes caught. Each EHT consisted of six experimental huts, with five insecticide treated nets (ITNs) and one untreated net tested. Study participants slept in the experimental huts six days a week. The study was conducted between the 8th of September and the 22 October 2014, with 36 sampling days (for one day per week there was no sampling). Differences between nets were ignored as the analysis used the number of mosquitoes caught per night and did not consider mosquito mortality or feeding status.

4.2. Individual based adult mosquito model

We develop the individual based model (IBM) to simulate adult female mosquito population dynamics over discrete time steps using the *individual* R package version 0.1.17 [55]. For all models and equations we assume a time step of size $dt = 1$ day, meaning the mosquito ages are limited to the nearest complete day. The model is stochastic and at each time step the number of emerging adult female mosquitoes, o_t, is,

$$o_t \sim \text{Poisson}(\lambda_t), \tag{1}$$

where $\lambda_t > 0$ varies over time t (in days). This model does, therefore, not allow feedback between the current mosquito population size and numbers of emerging adult female mosquitoes, but allows the impact of different types of variability in adult mosquito emergence to be isolated. Given $a>0$ is the constant per-mosquito biting rate per day, then the probability a mosquito has bitten during a single day is given by the exponential distribution cumulative distribution function (CDF): $1–e^{-a}$. Newly emerged mosquitoes are all nulliparous (*NP*), and the number of simulation time steps for completion of the first gonotrophic cycle, G_i, of each mosquito, i, is sampled,

$$G_i \sim \text{Geometric}(1 - e^{-a}). \tag{2}$$

Once the first gonotrophic cycle is complete mosquitoes transition to the parous, *P*, state. Following existing *Anopheles* population models and empirical inference [46], mosquitoes are assumed to die at a constant age-independent mortality rate, μ, such that at each time step individual mosquito survival, S_i is determined by,

$$S_i \sim \text{Bernoulli}(e^{-\mu}). \tag{3}$$

Dead mosquitoes are removed from the population, and at each time step the age of the individual mosquitoes is incremented by $dt = 1$. In existing continuous time malaria transmission models [37] it is assumed that the biting rate and mortality rate prior to the introduction of control interventions for *An. gambiae* are $a = \frac{1}{3}$ and $\mu = 0.132$ respectively. In the continuous time model where biting times and adults mosquito life expectancies are exponentially distributed these give mean times of 3 and 7.6 days respectively. Using the geometric distribution and binomial approximation to transition mosquitoes between time steps gives mean biting times and life expectancies of 2.5 and 7.1 days.

4.2.1. Simulation. The daily variability in adult mosquitoes emergence will depend on the geographical scale being considered in addition to the oviposition behaviour and bionomics of the mosquito (for example, whether a mosquito skip-oviposits or lays eggs in clumps). Variability in emergence from a single breeding site may be considerable, but this

heterogeneity could be dampened due to statistical averaging if adult mosquitoes from multiple distinct breeding sites are caught in the same trap (the portfolio effect) [43], which is not considered in our analyses. The impact of stochastic fluctuations will also depend on the size of the mosquito group considered. Here we consider a theoretical, dynamic group of adult female mosquitoes. To represent the underlying population structure the model outputs the age distribution of living mosquitoes at all time points, which is equivalent to collecting and age-grading all mosquitoes. We do not consider heterogeneity generated by the sampling process, for example caused by trapping biases or small sample sizes.

To assess the hypothetical impact of intra-annual changes in mosquito emergence, we characterised temporal changes in the adult mosquito emergence rate, λ_t, using a sine function;

$$\lambda_t = \bar{\lambda} + \eta \sin(2\pi\kappa t), \tag{4}$$

where $2\pi\kappa$ is the angular frequency, η is the amplitude and $\bar{\lambda}$ is the time invariant mean of the mean numbers of mosquitoes emerging. To ensure the population does not go extinct or increase exponentially, we set the mean number of births per day equal to the daily mortality probability multiplied by the initial number of mosquitoes (M_0); $\bar{\lambda} = M_0(1 - e^{-\mu})$. This ensures an average of 200 mosquitoes over each stimulation, though the number of mosquitoes changes over time according to the seasonality under consideration. The number of mosquitoes is approximately informed by the EHT data, where a median of 16 mosquitoes were caught per experimental hut during the transmission season, there are 6 experimental huts and it is assumed mosquitoes are only caught when attempting to blood-feed.

We assess temporal changes in the mosquito age distribution and parity given the following seasonality profiles:

1. no long-term changes in emergence ($\kappa = 0$), which is representative of perennial mosquito abundance, and,
2. a single peak per year ($\kappa = \frac{1}{365}$), which is representative of wet-dry season dynamics.

To investigate the sensitivity of the modelled age distribution to different amplitude fluctuations in mosquito emergence, for the single peak per year seasonality profile we simulate mosquito emergence with a range of amplitudes (η). To assess the effect of different phenomenological changes in mosquito emergence on the temporal variability in the daily mean mosquito age, we run the model with a range κ values corresponding to a frequencies between 1 and 50 radians per year with an amplitude (η) of 10. For these seasonal trends the sine wave frequencies corresponded to complete periods over a single year.

To model the effects of temporal variation in the mean adult mosquito emergence rate due to stochastic noise, for example due to hypothetical variation in a environmental variable [28], we apply a discrete-time lag-1 autoregressive model,

$$\lambda_{t+1} \sim \text{Normal}\left(\text{mean} = \bar{o} + h(\lambda_t - \bar{o}), \text{sd} = \sigma\sqrt{1 - h^2}\right), \tag{5}$$

where, $\bar{o}$ is the time-invariant fitted mean emergence rate (also assumed to be equal to $M_0(1 - e^{-\mu})$), h is the autocorrelation parameter and σ is the standard deviation. We generate stochastic changes in the emergence rate for the duration of the simulations for numerous values of $-0.9 \leq h \leq 0.9$ with a 1-day lag and three values of $\sigma \in (1, 3, 5)$. The $\bar{o}$ and σ values are selected such that λ is greater than zero.

For each parameter set for the frequency and autocorrelation sensitivity analyses the mosquito population dynamics are simulated 20 times for 5 years and the first 4 years

excluded. For each simulation we calculate the temporal variability in the mean mosquito age, abundance, proportion of mosquitoes at least 10 days old and parity over the final year, and quantify temporal variability in these values using the $CV = \frac{standard\ deviation}{mean}$.

To estimate the per-capita mortality rate from the mosquito age distributions, we add 10^{-5} to each age, such that no mosquitoes were aged zero, and fit a parametric survival model to the mosquito ages using the R survival package [56], assuming a constant per-capita mortality rate, exponential distribution and mosquitoes die at their current age.

This model was used to generate the plots presented in Figs 1, 2D, 2E and S4 Fig-S7 Fig.

4.3. Estimating the autocorrelation in the emergence rate of wild mosquito populations

To estimate autocorrelation in the emergence of wild mosquito populations from mosquito abundance data, we fit an ordinary differential equation (ODE) based mosquito population model to EHT data. Age distribution data are not available for these mosquitoes. To identify the autocorrelation in the temporal trends in mosquito emergence, we fit an ODE mosquito population model, with the same assumptions about mosquito survival and mortality, to the numbers of mosquitoes caught per experimental hut, m, irrespective of mortality and blood-feeding status. In EHTs, interventions and sleepers can correlate with differences in the total number of mosquitoes caught, but interventions and sleepers are rotated between experimental huts in a fully factorial design, so we do not explicitly account for these variables when estimating the temporal dynamics of mosquito emergence. We assume temporal changes in mosquitoes numbers, M, are determined by temporal changes in mosquito emergence only meaning,

$$\frac{dM}{dt} = \lambda(t) - \mu M. \tag{6}$$

EHTs occur over relatively short timescales and mark-release-recapture studies indicate a lack of evidence for senescence in wild mosquitoes [46], so we assume a constant per-capita mosquito mortality rate of $\mu = 0.132$, in line with existing malaria transmission models [37]. Integrating Eq 6 with the assumption that the population-level emergence rate $\lambda(t)$ is constant within each day gives,

$$M_{t+1} = \frac{e^{-\mu}(M_t\mu + \lambda(t)(e^{\mu} - 1))}{\mu}; \tag{7}$$

We fit this model in a Bayesian framework assuming the daily mosquito counts per experimental hut are negative binomial distributed;

$$m_t \sim \mathrm{NB}(\mathrm{mean} = M_t, \mathrm{overdispersion} = \phi), \tag{8}$$

where ϕ is the overdispersion parameter, such that $var[m_t] = \frac{M_t}{\phi}(\phi + 1)$. $\lambda(t)$ is the time-dependent mosquito emergence rate per day in the population as a whole and does not depend on the current mosquito population size; this quantity was fitted hierarchically using the lag-1 autoregressive model described in Eq 5.

For each EHT, the posterior distributions of M_0, λ_t, ϕ, h and σ are estimated using the No U-turn Markov chain Monte Carlo (MCMC) sampler from Stan [57]. Wide normal priors are assumed: $M_0 \sim \mathrm{N}(15, 2.5)$, $\phi \sim \mathrm{N}(1, 2.5)$, $h \sim \mathrm{N}(0, 1)$ and $\sigma \sim \mathrm{N}(0.5, 2.5)$. Convergence

is assessed by visualising the trace plots and $\hat{R} < 1.01$ for all parameters. Results of the model fitting are presented in Fig 2A–2C, with fitted parameter values shown in S8 Fig.

We then simulate mosquito population dynamics using the IBM given the estimated constant daily emergence rates ($\lambda(t)$) and initial numbers of mosquitoes (M_0) from the EHTs. To do so, we multiply the fitted λ_t and M_0 by the number of experimental huts to account for the mosquitoes in each experimental hut and inputted these values directly into the IBM. These results are presented in Fig 2D and 2E.

4.4. Compartmental mosquito model with ITNs

To model the effects of pyrethroid-only ITNs on the adult mosquito age distribution we use the *odin* and *odin.dust* R packages [58] to develop a discrete time stochastic compartmental approximation of an established differential equation larval and adult mosquito population model used in malaria transmission modelling [36–38]. Unlike the model outlined in Eqs 1–5 this model does not track individual mosquitoes but links the number of eggs and juvenile stages to the number of adult female mosquitoes. Within this model mosquitoes are classed as early stage larvae (E) late stage larvae (L), pupae (P) and female adult mosquitoes (A). We adapt this model, such that at each time step ($dt = 1$) the time-dependent numbers of births of new larvae is,

$$n_{b,t} \sim \text{Poisson}(A_t \beta_t), \tag{9}$$

where β_t is the number of eggs laid per day per mosquito and A_t is the number of adult mosquitoes on day t (S1 Text). Male and female larval population dynamics are density dependent with the time-dependent changes in the mortality rates and carrying capacity, $K(t)$,

$$\begin{aligned} \mu_{E,t} &= \mu_e\left(1 + \frac{E_t + L_t}{K(t)}\right), \\ \mu_{L,t} &= \mu_l \gamma\left(1 + \frac{E_t + L_t}{K(t)}\right), \end{aligned} \tag{10}$$

where $\mu_e = 0.0338$ and $\mu_l = 0.0348$ per-day are the per-capita daily mortality rates of early stage larvae and late stage larvae respectively. $\mu_p = 0.249$ is the pupae mortality rate. Seasonality in the population dynamics occurs due to seasonal changes in the carrying capacity (S1 Text). Mosquitoes also transition due to development to other life stages; $d_{el} = 6.64$, $d_l = 3.72$ and $d_p = 0.643$ days are the development times of early stage larvae, late stage larvae and pupae respectively [36]. We assume these rates are constant over a single time step and calculated the probability an event (death or development) for each life stage has occurs during that time step using an exponential CDF. The total rates of removal from each stage including both mortality and transition to other life stages were calculated as,

$$\begin{aligned} \alpha_{E,t} &= \mu_{E,t} + \frac{1}{d_{el}}, \\ \alpha_{L,t} &= \mu_{L,t} + \frac{1}{d_l}, \\ \alpha_P &= \mu_p + \frac{1}{d_p}. \end{aligned} \tag{11}$$

The numbers of mosquitoes that transition at each time step are then sampled thus,

$$\begin{aligned} n_{E,t} &\sim \text{Binomial}(E_t, 1 - e^{\alpha_{E,t}}), \\ n_{EL,t} &\sim \text{Binomial}(n_{E,t}, \frac{1}{\alpha_{E,t} d_{el}}) \\ n_{L,t} &\sim \text{Binomial}(L_t, 1 - e^{\alpha_{L,t}}) \\ n_{LP,t} &\sim \text{Binomial}(n_{L,t}, \frac{1}{\alpha_{L,t} d_l}) \\ n_{P,t} &\sim \text{Binomial}(P_t, 1 - e^{\alpha_P}), \end{aligned} \tag{12}$$

where $n_{E,t}$, $n_{L,t}$ and $n_{P,t}$ are the numbers leaving the early larvae, late larve and pupae life stage compartments respectively; $n_{EL,t}$ and $n_{LP,t}$ are the numbers transitioning to the late larvae and pupae life stages respectively. Note that to calculate the numbers that develop to the next life stage and do not die we take a binomial sample from the total number transitioning with the probability determined by the proportion of the total rate account for by the development rate. The larval population dynamics are then calculated as,

$$\begin{aligned} E_{t+1} &= E_t + n_{b,t} - n_{E,t}, \\ L_{t+1} &= L_t + n_{EL,t} - n_{L,t} \\ P_{t+1} &= P_t + n_{LP,t} - n_{P,t}. \end{aligned} \tag{13}$$

The adult female mosquito, A, compartments were stratified by age in time-steps; where $A_{j,t}$, denotes the number of mosquitoes aged j (in dt) at time t. The ageing process is calculated thus,

$$\begin{aligned} n_{PA,t} &\sim \text{Binomial}(n_{P,t}, \frac{1}{\alpha_P d_p}), \\ A_{0,t+1} &\sim \text{Binomial}(n_{PA,t}, \frac{1}{2}), \\ n_{A_{0,t}} &\sim \text{Binomial}(A_{0,t}, 1 - e^{-\mu_t}), \\ A_{1,t+1} &= A_{0,t} - n_{A_0,t}, \\ &\ldots \\ n_{A_{j-1,t}} &\sim \text{Binomial}(A_{j-1,t}, 1 - e^{-\mu_t}), \\ A_{j,t+1} &= A_{j-1,t} - n_{A_{j-1,t}}, \end{aligned} \tag{14}$$

where μ_t is the per-capita adult mosquito mortality rate, which depends on the presence of ITNs (S1 Text). Note that the number of pupae developing into adults is drawn from a binomial sample with a $\frac{1}{2}$ probability because only female adult mosquitoes are modelled.

In this analysis, we assume a population ITN usage of 0 or 100%, which does not change over time and an ITN entomological efficacy observed for pyrethroid-only ITNs with a mosquito population that is susceptible to pyrethroid insecticide (i.e. prior to the development of pyrethroid resistance) (S1 Text), assuming there is no insecticide resistance, 100% ITN coverage, and the proportions of anthropophagy (equal to 0.92), bites indoors (equal to 0.97) and bites when people are in bed (equal to 0.89) are high. This model is presented in Fig 3.

Supporting information

S1 Text. Compartmental mosquito model supplementary methods.
(PDF)

S1 Fig. Seasonal dynamics in mosquito abundance with a range of different frequencies in mosquito emergence. Facet show the period of the sine wave per year (multiplied by 365; 365κ). The amplitude of adult mosquito emergence was assumed to be constant at 10 mosquitoes, which is approximately 40% of the mean emergence rate mean ($\frac{100\eta}{o}$).
(TIFF)

S2 Fig.Seasonal dynamics in mosquito abundance with a range of different amplitudes in mosquito emergence. Facet show the amplitude as a percent of the mean emergence rate mean ($\frac{100\eta}{o}$). The frequency of adult mosquito emergence was assumed to be constant with a single peak per year.
(TIFF)

S3 Fig. The theoretical effect of different (A) frequency and (B) amplitude changes in mosquito emergence on the temporal variability in the mean mosquito age. (A) Mosquito emergence was simulated to fluctuate according to a sine wave with the number of periods per year. The mean mosquito emergence was assumed to be equal to the initial mosquito population size multiplied by the daily probability of mortality. An amplitude of 10 is assumed, which is approximately 40% of the mean of the mean emergence rate ($\bar{o}$). (B) The temporal variability in the daily mean mosquito age given different amplitude fluctuations in the mean mosquito emergence rate and a frequency (365κ) of 1 radians per year. For (A) and (B) boxplots show the variability between different simulations with the ggplot2 default parameters (the box shows the 25%, 50% and 75% quantiles).
(TIFF)

S4 Fig. Seasonal dynamics in the per-capita mosquito mortality rate estimated from temporal changes in the mosquito age distributions. The pink/purple lines show the results where the mosquito populations is simulated with an adult mosquito emergence rate that follows a sine wave with a single period per year and the yellow lines show those with perennial mosquito population dynamics. The thin lines show the results from a single simulation and the thicker lines show the mean values of all the simulations.
(TIFF)

S5 Fig. The theoretical impact of autocorrelation in emergence mosquito abundance abundance and age. (A) The theoretical noise in the mean mosquito emergence rate (λ_t) for a single year for a single simulation, given a lag-1 autoregressive model with the same mean and standard deviation but different levels of autocorrelation (h). (B) The temporal dynamics of mosquito abundance (black) and newly emerged mosquitoes (between 0 and 1 day old) corresponding to the λ_t values in A. (C) The distribution of the simulated mean daily ages over a single year given different levels of autocorrelation. Temporal variability in the mean ages is presented as a density because different simulations with the same autocorrelation parameters do not necessarily shows the same trends at the same time. The density was estimated from the the frequencies of the mosquito ages using a Gaussian kernel. For all plots the mean of the mean emergence rate (o) was assumed to be (26.4) and the standard deviation (σ) 5 in the lag-1 autoregressive model.
(TIFF)

S6 Fig. Seasonal dynamics in mosquito abundance with a range of different autocorrelations in mosquito emergence. Facet columns show the standard deviation (σ) and facet rows show the autocorrelation (h). Values are shown for a single simulation.
(TIFF)

S7 Fig. The effects of different levels of autocorrelation in the mean emergence rate (λ_t given a lag-1 autoregressive model with different autocorrelation (h) and standard deviation (σ) parameters on the coefficient of variation in the mean daily mosquito ages over a single year. Boxplots show the variability between different simulations with the ggplot2 default parameters (the box shows the 25%, 50% and 75% quantiles).
(TIFF)

S8 Fig. Posterior densities of (A) the lag-1 regression model of the mosquito emergence rate mean for the ODE model, (B) the standard deviation of the lag-1 regression model of the mean mosquito emergence rate and (C) the negative binomial overdispersion parameter from fitting this model to the EHT data.
(TIFF)

Acknowledgments

The authors would like to thank Nakul Chitnis and Maria-Gloria Basáñez for comments on early versions of the work.

Author contributions

Conceptualization: Isaac J. Stopard, Ellie Sherrard-Smith, Hilary Ranson, Ben Lambert, Thomas S. Churcher.

Data curation: Isaac J. Stopard, Hilary Ranson, Kobié Hyacinthe Toe.

Formal analysis: Isaac J. Stopard.

Funding acquisition: Isaac J. Stopard, Jackie Cook, Joseph Biggs, Thomas S. Churcher.

Investigation: Isaac J. Stopard.

Methodology: Isaac J. Stopard, Ellie Sherrard-Smith, Ben Lambert, Thomas S. Churcher.

Software: Isaac J. Stopard.

Supervision: Ben Lambert, Thomas S. Churcher.

Validation: Ellie Sherrard-Smith.

Visualization: Isaac J. Stopard.

Writing – original draft: Isaac J. Stopard, Ellie Sherrard-Smith, Ben Lambert, Thomas S. Churcher.

Writing – review & editing: Isaac J. Stopard, Ellie Sherrard-Smith, Hilary Ranson, Kobié Hyacinthe Toe, Jackie Cook, Joseph Biggs, Ben Lambert, Thomas S. Churcher.

References

1. Tusting LS, Bousema T, Smith DL, Drakeley C. Measuring changes in Plasmodium falciparum transmission: precision, accuracy and costs of metrics. Adv Parasitol. 2014;84:151–208. https://doi.org/10.1016/B978-0-12-800099-1.00003-X PMID: 24480314

2. Van Hul N, Braks M, Van Bortel W. A systematic review to understand the value of entomological endpoints for assessing the efficacy of vector control interventions. EFS3. 2021;18(11). https://doi.org/10.2903/sp.efsa.2021.EN-6954
3. Wong J, Bayoh N, Olang G, Killeen GF, Hamel MJ, Vulule JM, et al. Standardizing operational vector sampling techniques for measuring malaria transmission intensity: evaluation of six mosquito collection methods in western Kenya. Malar J. 2013;12:143. https://doi.org/10.1186/1475-2875-12-143 PMID: 23631641
4. Reiner RC Jr, Guerra C, Donnelly MJ, Bousema T, Drakeley C, Smith DL. Estimating malaria transmission from humans to mosquitoes in a noisy landscape. J R Soc Interface. 2015;12(111):20150478. https://doi.org/10.1098/rsif.2015.0478 PMID: 26400195
5. Suh E, Stopard IJ, Lambert B, Waite JL, Dennington NL, Churcher TS, et al. Estimating the effects of temperature on transmission of the human malaria parasite, Plasmodium falciparum. Nat Commun. 2024;15(1):3230. https://doi.org/10.1038/s41467-024-47265-w PMID: 38649361
6. Chan M, Johansson MA. The incubation periods of Dengue viruses. PLoS One. 2012;7(11):e50972. https://doi.org/10.1371/journal.pone.0050972 PMID: 23226436
7. Macdonald G. Epidemiological basis of malaria control. Bull World Health Organ. 1956;15(3–5):613–26. PMID: 13404439
8. Smith DL, McKenzie FE. Statics and dynamics of malaria infection in Anopheles mosquitoes. Malar J. 2004;3:13. https://doi.org/10.1186/1475-2875-3-13 PMID: 15180900
9. Joy TK, Jeffrey Gutierrez EH, Ernst K, Walker KR, Carriere Y, Torabi M, et al. Aging field collected Aedes aegypti to determine their capacity for dengue transmission in the southwestern United States. PLoS One. 2012;7(10):e46946. https://doi.org/10.1371/journal.pone.0046946 PMID: 23077536
10. Bhatt S, Weiss DJ, Cameron E, Bisanzio D, Mappin B, Dalrymple U, et al. The effect of malaria control on Plasmodium falciparum in Africa between 2000 and 2015. Nature. 2015;526(7572):207–11. https://doi.org/10.1038/nature15535 PMID: 26375008
11. Erlanger TE, Keiser J, Utzinger J. Effect of dengue vector control interventions on entomological parameters in developing countries: a systematic review and meta-analysis. Med Vet Entomol. 2008;22(3):203–21. https://doi.org/10.1111/j.1365-2915.2008.00740.x PMID: 18816269
12. Johnson BJ, Hugo LE, Churcher TS, Ong OTW, Devine GJ. Mosquito age grading and vector-control programmes. Trends in Parasitology. 2020;36(1):39–51. https://doi.org/10.1016/j.pt.2019.10.011
13. Detinova TS, Bertram DS, Organization WH. Age-grouping methods in Diptera of medical importance, with special reference to some vectors of malaria. World Health Organization; 1962.
14. Killeen GF, McKenzie FE, Foy BD, Schieffelin C, Billingsley PF, Beier JC. A simplified model for predicting malaria entomologic inoculation rates based on entomologic and parasitologic parameters relevant to control. Am J Trop Med Hyg. 2000;62(5):535–44. https://doi.org/10.4269/ajtmh.2000.62.535 PMID: 11289661
15. Schlein Y, Gratz NG. Determination of the age of some anopheline mosquitos by daily growth layers of skeletal apodemes. Bull World Health Organ. 1973;49(4):371–5. PMID: 4368577
16. Siria DJ, Sanou R, Mitton J, Mwanga EP, Niang A, Sare I, et al. Rapid age-grading and species identification of natural mosquitoes for malaria surveillance. Nat Commun. 2022;13(1):1501. https://doi.org/10.1038/s41467-022-28980-8 PMID: 35314683
17. Gao Z, Harrington LC, Zhu W, Barrientos LM, Alfonso-Parra C, Avila FW, et al. Accurate age-grading of field-aged mosquitoes reared under ambient conditions using surface-enhanced Raman spectroscopy and artificial neural networks. J Med Entomol. 2023;60(5):917–23. https://doi.org/10.1093/jme/tjad067 PMID: 37364175
18. Robert V, Carnevale P. Influence of deltamethrin treatment of bed nets on malaria transmission in the Kou valley, Burkina Faso. Bull World Health Organ. 1991;69(6):735–40. PMID: 1786622
19. Smith DL, Dushoff J, McKenzie FE. The risk of a mosquito-borne infection in a heterogeneous environment. PLoS Biol. 2004;2(11):e368. https://doi.org/10.1371/journal.pbio.0020368 PMID: 15510228
20. Parra MCP, Lorenz C, Dibo MR, de Aguiar Milhim BHG, Guirado MM, Nogueira ML, et al. Association between densities of adult and immature stages of Aedes aegypti mosquitoes in space and time: implications for vector surveillance. Parasit Vectors. 2022;15(1):133. https://doi.org/10.1186/s13071-022-05244-4 PMID: 35440010
21. Koenraadt CJM, Githeko AK, Takken W. The effects of rainfall and evapotranspiration on the temporal dynamics of Anopheles gambiae s.s. and Anopheles arabiensis in a Kenyan village. Acta Trop. 2004;90(2):141–53. https://doi.org/10.1016/j.actatropica.2003.11.007 PMID: 15177140
22. Fontenille D, Lochouarn L, Diagne N, Sokhna C, Lemasson JJ, Diatta M, et al. High annual and seasonal variations in malaria transmission by anophelines and vector species composition in

Dielmo, a holoendemic area in Senegal. Am J Trop Med Hyg. 1997;56(3):247–53. https://doi.org/10.4269/ajtmh.1997.56.247 PMID: 9129525

23. Bjørnstad ON, Grenfell BT. Noisy clockwork: time series analysis of population fluctuations in animals. Science. 2001;293(5530):638–43. https://doi.org/10.1126/science.1062226
24. Lande R, Engen S, Saether BE. Stochastic population dynamics in ecology and conservation. Oxford University Press on Demand; 2003.
25. Boyce MS, Haridas CV, Lee CT, The Nceas Stochastic Demography Working Group. Demography in an increasingly variable world. Trends Ecol Evol. 2006;21(3):141–8. https://doi.org/10.1016/j.tree.2005.11.018 PMID: 16701490
26. Kaitala V, Ylikarjula J, Ranta E, Lundberg P. Population dynamics and the colour of environmental noise. Proc Biol Sci. 1997;264(1384):943–8. https://doi.org/10.1098/rspb.1997.0130 PMID: 9304115
27. Inchausti P, Halley J. The long-term temporal variability and spectral colour of animal populations. Evolutionary Ecology Research. 2002;4(7):1033–48.
28. Ruokolainen L, Lindén A, Kaitala V, Fowler MS. Ecological and evolutionary dynamics under coloured environmental variation. Trends Ecol Evol. 2009;24(10):555–63. https://doi.org/10.1016/j.tree.2009.04.009 PMID: 19699550
29. Petchey OL. Environmental colour affects aspects of single-species population dynamics. Proc Biol Sci. 2000;267(1445):747–54. https://doi.org/10.1098/rspb.2000.1066 PMID: 10819142
30. Whittaker C, Winskill P, Sinka M, Pironon S, Massey C, Weiss DJ, et al. A novel statistical framework for exploring the population dynamics and seasonality of mosquito populations. Proc Biol Sci. 2022;289(1972):20220089. https://doi.org/10.1098/rspb.2022.0089 PMID: 35414241
31. Parham PE, Pople D, Christiansen-Jucht C, Lindsay S, Hinsley W, Michael E. Modeling the role of environmental variables on the population dynamics of the malaria vector Anopheles gambiae sensu stricto. Malar J. 2012;11:271. https://doi.org/10.1186/1475-2875-11-271 PMID: 22877154
32. Zhou G, Munga S, Minakawa N, Githeko AK, Yan G. Spatial relationship between adult malaria vector abundance and environmental factors in western Kenya highlands. Am J Trop Med Hyg. 2007;77(1):29–35. PMID: 17620627
33. Minakawa N, Sonye G, Mogi M, Githeko A, Yan G. The effects of climatic factors on the distribution and abundance of malaria vectors in Kenya. J Med Entomol. 2002;39(6):833–41. https://doi.org/10.1603/0022-2585-39.6.833 PMID: 12495180
34. Munga S, Yakob L, Mushinzimana E, Zhou G, Ouna T, Minakawa N, et al. Land use and land cover changes and spatiotemporal dynamics of anopheline larval habitats during a four-year period in a highland community of Africa. Am J Trop Med Hyg. 2009;81(6):1079–84. https://doi.org/10.4269/ajtmh.2009.09-0156
35. Toe KH, Müller P, Badolo A, Traore A, Sagnon N, Dabiré RK, et al. Do bednets including piperonyl butoxide offer additional protection against populations of Anopheles gambiae s.l. that are highly resistant to pyrethroids? An experimental hut evaluation in Burkina Fasov. Med Vet Entomol. 2018;32(4):407–16. https://doi.org/10.1111/mve.12316 PMID: 29998497
36. White MT, Griffin JT, Churcher TS, Ferguson NM, Basáñez M-G, Ghani AC. Modelling the impact of vector control interventions on Anopheles gambiae population dynamics. Parasit Vectors. 2011;4:153. https://doi.org/10.1186/1756-3305-4-153 PMID: 21798055
37. Griffin JT, Hollingsworth TD, Okell LC, Churcher TS, White M, Hinsley W, et al. Reducing Plasmodium falciparum malaria transmission in Africa: a model-based evaluation of intervention strategies. PLoS Med. 2010;7(8):e1000324. https://doi.org/10.1371/journal.pmed.1000324 PMID: 20711482
38. Challenger JD, Olivera Mesa D, Da DF, Yerbanga RS, Lefèvre T, Cohuet A, et al. Predicting the public health impact of a malaria transmission-blocking vaccine. Nat Commun. 2021;12(1):1494. https://doi.org/10.1038/s41467-021-21775-3 PMID: 33686061
39. Gillies MT, Wilkes TJ. A study of the age-composition of populations of Anopheles gambiae Giles and A. funestus Giles in North-Eastern Tanzania. Bull Entomol Res. 1965;56(2):237–62. https://doi.org/10.1017/s0007485300056339 PMID: 5854754
40. Challenger JD, Nash RK, Ngufor C, Sanou A, Toé KH, Moore S, et al. Assessing the variability in experimental hut trials evaluating insecticide-treated nets against malaria vectors. Curr Res Parasitol Vector Borne Dis. 2023;3:100115. https://doi.org/10.1016/j.crpvbd.2023.100115 PMID: 36895438
41. Jian Y, Silvestri S, Brown J, Hickman R, Marani M. The temporal spectrum of adult mosquito population fluctuations: conceptual and modeling implications. PLoS One. 2014;9(12):e114301. https://doi.org/10.1371/journal.pone.0114301 PMID: 25478861
42. Lutambi AM, Penny MA, Smith T, Chitnis N. Mathematical modelling of mosquito dispersal in a heterogeneous environment. Math Biosci. 2013;241(2):198–216.

https://doi.org/10.1016/j.mbs.2012.11.013 PMID: 23246807

43. Killeen GF, Reed TE. The portfolio effect cushions mosquito populations and malaria transmission against vector control interventions. Malar J. 2018;17(1). https://doi.org/10.1186/s12936-018-2441-z
44. Dawes EJ, Churcher TS, Zhuang S, Sinden RE, Basáñez M-G. Anopheles mortality is both age- and Plasmodium-density dependent: implications for malaria transmission. Malar J. 2009;8:228. https://doi.org/10.1186/1475-2875-8-228 PMID: 19822012
45. Ryan SJ, Ben-Horin T, Johnson LR. Malaria control and senescence: the importance of accounting for the pace and shape of aging in wild mosquitoes. Ecosphere. 2015;6(9):1–13. https://doi.org/10.1890/es15-00094.1
46. Lambert B, North A, Godfray HCJ. A meta-analysis of longevity estimates of mosquito vectors of disease. Cold Spring Harbor Laboratory; 2022. https://doi.org/10.1101/2022.05.30.494059
47. Bayoh MN. Studies on the development and survival of Anopheles gambiae sensu stricto at various temperatures and relative humidities. 2001.
48. Ngowo HS, Okumu FO, Hape EE, Mshani IH, Ferguson HM, Matthiopoulos J. Using Bayesian state-space models to understand the population dynamics of the dominant malaria vector, Anopheles funestus in rural Tanzania. Malar J. 2022;21(1):161. https://doi.org/10.1186/s12936-022-04189-4 PMID: 35658961
49. Epopa PS, Millogo AA, Collins CM, North A, Tripet F, Benedict MQ, et al. The use of sequential mark-release-recapture experiments to estimate population size, survival and dispersal of male mosquitoes of the Anopheles gambiae complex in Bana, a west African humid savannah village. Parasites & Vectors. 2017;10(1):376. https://doi.org/10.1186/s13071-017-2310-6
50. Blanford S, Read AF, Thomas MB. Thermal behaviour of Anopheles stephensi in response to infection with malaria and fungal entomopathogens. Malar J. 2009;8:72. https://doi.org/10.1186/1475-2875-8-72 PMID: 19379519
51. Paaijmans KP, Thomas MB. The influence of mosquito resting behaviour and associated microclimate for malaria risk. Malar J. 2011;10:183. https://doi.org/10.1186/1475-2875-10-183 PMID: 21736735
52. Ngowo HS, Kaindoa EW, Matthiopoulos J, Ferguson HM, Okumu FO. Variations in household microclimate affect outdoor-biting behaviour of malaria vectors. Wellcome Open Res. 2017;2:102. https://doi.org/10.12688/wellcomeopenres.12928.1 PMID: 29552642
53. Msugupakulya BJ, Kaindoa EW, Ngowo HS, Kihonda JM, Kahamba NF, Msaky DS, et al. Preferred resting surfaces of dominant malaria vectors inside different house types in rural south-eastern Tanzania. Malar J. 2020;19(1):22. https://doi.org/10.1186/s12936-020-3108-0 PMID: 31941508
54. Briët OJT. A simple method for calculating mosquito mortality rates, correcting for seasonal variations in recruitment. Med Vet Entomol. 2002;16(1):22–7. https://doi.org/10.1046/j.0269-283x.2002.00335.x PMID: 11963978
55. Charles G, Wu S. individual: an R package for individual-based epidemiological models. JOSS. 2021;6(66):3539. https://doi.org/10.21105/joss.03539
56. Therneau TM. A Package for Survival Analysis in R. 2024.
57. Carpenter B, Gelman A, Hoffman MD, Lee D, Goodrich B, Betancourt M, et al. Stan: a probabilistic programming language. J Stat Softw. 2017;76:1. https://doi.org/10.18637/jss.v076.i01 PMID: 36568334
58. FitzJohn R, Hill A, Lees J. Odin.dust: compile odin to dust. 2024. https://github.com/mrc-ide/odin.dust